UNCERTAINTY OF NIST AIRSPEED CALIBRATIONS

T. T. Yeh
National Institute of Standards and Technology
100 Bureau Drive
Gaithersburg, MD 20899
(301)975-5953
ttyeh@nist.gov

J. M. Hall
National Institute of Standards and Technology
100 Bureau Drive
Gaithersburg, MD 20899
(301)975-5947
mikehall@nist.gov

Abstract - The National Institute of Standards and Technology (NIST) provides calibration services for airspeed instruments. Here, we describe NIST's recently upgraded airspeed calibration system and its uncertainty. At NIST, airspeed calibrations are performed over the range 0.15 m/s to 40 m/s in the wind tunnel that has a test cross section of 1.5 m by 2.1 m. The standard for airspeed measurement is a fiber optic laser Doppler anemometer (LDA), which is calibrated with known velocities produced by a rotating disk. The expanded airspeed uncertainty at 95 % confidence level (i.e. coverage factor k=2) in m/s is the root-sum-square of 0.0064V and 0.0036 m/s, where V is airspeed in m/s. This gives a maximum uncertainty of 2.5 % (0.0038 m/s) at the lowest airspeed of 0.15 m/s and a minimum uncertainty of 0.65 % (0.26 m/s) at the highest speed of 40 m/s.

INTRODUCTION

The National Institute of Standards and Technology (NIST) provides calibration services for airspeed instrumentation such as Pitot-static tubes, anemometers (hot-wire, cup, and propeller types) as well as others. These calibration services provide traceability with a calibration report that documents the calibration procedure, the calibration results, and their uncertainties for airspeed sensor manufacturers, secondary airspeed calibration laboratories, and sensor users. The customer may use the sensor and its calibration results in different ways. It is often used as a transfer standard to compare the customer's primary standards to the NIST primary standards so that the customer can establish traceability, validate their uncertainty analysis, and demonstrate proficiency. Customers with no primary standards use their NIST calibrated airspeed sensors as working standards or reference standards in their laboratory to calibrate other airspeed sensors.

NIST has recently upgraded its hardware and reduced the uncertainty of the calibration measurements. The major upgrade of the system includes the replacements of a Laser unit, an improved air-water spraying nozzle system and a new laser Doppler anemometer (LDA) signal processor. This paper describes the upgrades and reports the uncertainty of the new NIST airspeed standards.

NIST's airspeed calibration system consists of a dual test section wind tunnel and a LDA airspeed measurement system. The airspeed is measured with a Dantec LDA*. A Pitot-static tube probe and thermal anemometer are used as check standards during every calibration. Routine calibrations are conducted by direct comparison of the averaged response of the instrument under test (IUT) with the response of the NIST LDA standard in the same air stream.

* The identification of any commercial product or trade name does not imply endorsement or recommendation by the National Institute of Standards and Technology.

Airspeed Calibration Facilities

NIST airspeed calibrations are conducted in a dual section wind tunnel [1] as shown in Fig. 1. The tunnel is a closed-circuit facility lying in a horizontal plane and has two interchangeable test sections. These two test section ducts ride "piggy back" on a cable hoisting arrangement. The upper test section is 12 m long and its normal dimensions of the cross-section are 2.1 m high and 1.5 m wide. The top speed in the upper test section is 45 m/s.

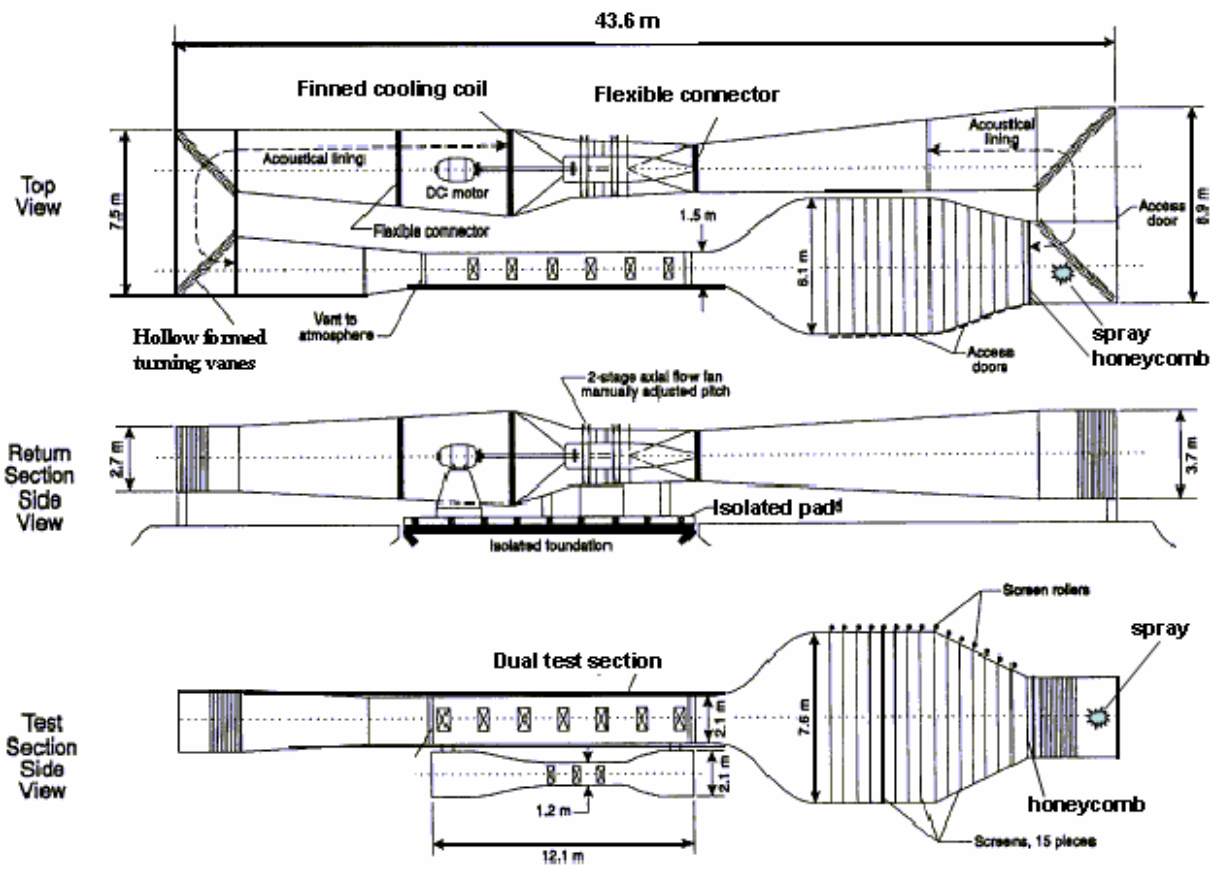

Figure 1 NIST Wind Tunnel for Airspeed Calibration Service.

In the lower test section, the 2.1 m height at the entrance is gradually reduced in the flow direction to 1.2 m forming a venturi-like duct so that the top speed is 67 m/s. The effective working length is 3.0 m within the overall 12 m length. Currently the airspeed calibrations are done only in the upper test section over a range of 0.15 m/s to 40 m/s. NIST is working to incorporate additional setups (e.g. a better seeding condition) so that the airspeed calibration service will reach 67 m/s.

The downstream end of each test section is vented to the room thereby establishing this point in the circuit near atmospheric pressure. From the test section, the flow passes into a 5º diffuser, around two 90º bends containing turning vanes, and into the drive section which measures 3.8 m by 4.4 m at the location of a cooling coil used to stabilize the tunnel temperature. A rectangular-to-round transition section makes the connection to the drive fan inlet. The entire drive mechanism, along with the cooling coil, is mounted on a large concrete slab, which is isolated from the building floor with springs to minimize the transmission of vibration. The main tunnel duct is attached to the drive section at each end by means of flexible boots.

The fan is powered by a variable speed 300 kW DC motor. The fan speed is controlled by a feedback loop that stabilizes the rotation rate within ±0.1%. The fan is 2.4 m in diameter with two axial stages and manually adjustable-pitch blades. Downstream of the fan the flow passes through a circular-to-square transition section and into a five-degree diffuser followed by the two more special diffusers sets. The upstream diffuser consists of two sets of turning vanes, a 1 cm by 7.6 cm honeycomb, and the downstream wide-angle diffuser containing 6 screens. After the diffuser, there is a 6.1 m by 7.5 m settling chamber having 9 screens. From the settling chamber the airflow passes through an entrance cone and into the 1.5 m by 2.1 m test section.

The combined effects of the honeycomb, screens, and a contraction ratio of 14.5:1 provide test section longitudinal free-stream turbulence levels of 0.07 % over most of the speed range and a transverse velocity gradient less than 1 % within a "working window" of 90 % of the test-section areas [1].

To provide the light scattering particles necessary for the operation of the LDA, water droplets, produced by several fine air-water spray nozzles, are introduced into the tunnel before the wide-angle diffuser and directed toward the honeycomb. (See Fig. 1 for the nozzle location.) Fig. 2 shows the fine water droplets with the spray nozzles. The spray is adjusted to optimize the data rate for the LDA signal processor.

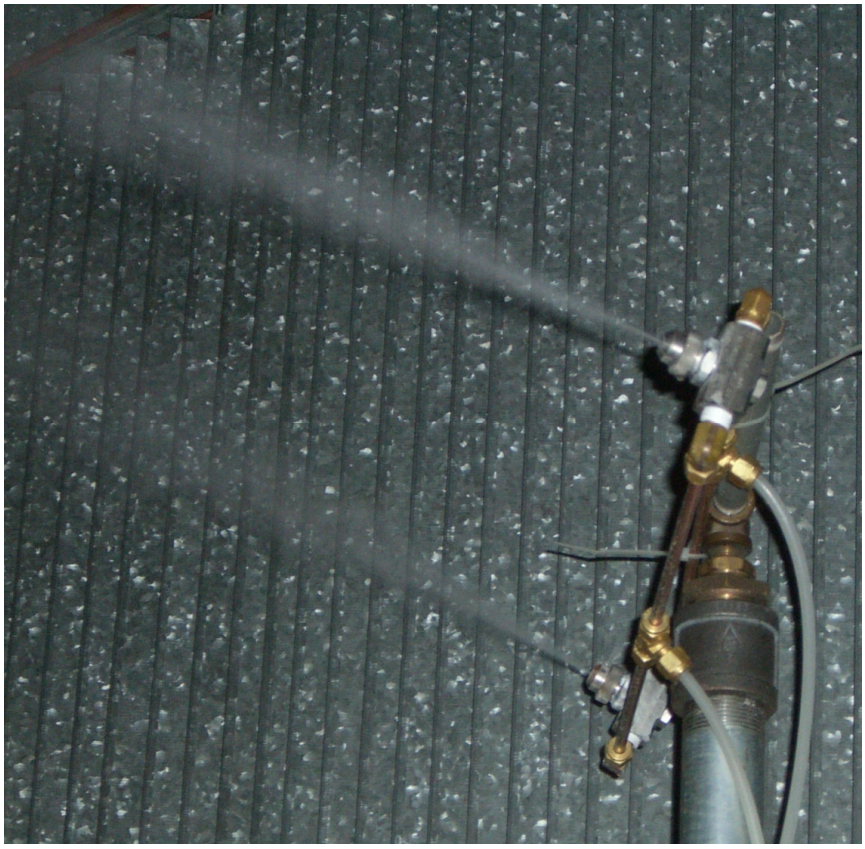

Figure 2 Photo of Fine Water Droplets With the Air-water Spray Nozzles

Primary Airspeed Standard -- LDA

The primary standard for airspeed measurement at NIST is a fiber optic LDA. This instrument has been characterized by calibrating its indicated speed using particles of known speed as discussed below.

Operation Principle of Laser Doppler Anemometry

An LDA measures the velocity of a particle moving in a plane perpendicular to the bisecting plane of the two converging laser beams [2, 3]. The NIST LDA system operates in a differential mode that modulates the light scattered by water droplets at the Doppler frequency and uses the modulation to measure the average droplet speed. The NIST LDA splits a laser beam into two beams in a plane and then recombines them at a small intersection angle θ by using a transmitting focus lens. In the intersection volume, the two beams are mutually coherent, collimated of like polarization and of equal intensity. The interaction between these two laser beams results in a three-dimensional region (sensing volume) which contains an interference pattern that is composed of parallel light and dark fringes. Small droplets, entrained in, and moving at the same speed as the air stream, scatter light as they pass through each bright fringe in the intersection volume. The NIST LDA operates in a backscattering configuration. Scattered light from the droplets moving through the fringe pattern is collected by the same lens used to transmit the two laser beams and focused onto a fiber detector. Because of the periodic fringe pattern, the scattered light will be intensity modulated at a frequency proportional to the component of the particle velocity perpendicular to the fringe pattern. The correct airspeed is measured when the probe is properly aligned such that the bisecting plane of the two laser beams is perpendicular to the direction of the flow.

The spacing between the bright fringes, d depends on the angle θ between the two laser beams and the laser wavelength λ as

$$d = \frac{\lambda}{2\sin\left(\frac{\theta}{2}\right)} \tag{1}$$

As shown in Fig. 3, when two parallel beams having a separation of *h* are combined by a lens having a focal length of f_L, the beams intersect at the angle

$$\theta = 2\tan^{-1}\left(\frac{h}{2f_L}\right) \tag{2}$$

In the context of airspeed measurement, the spacing d between the bright fringes serves as the length scale.

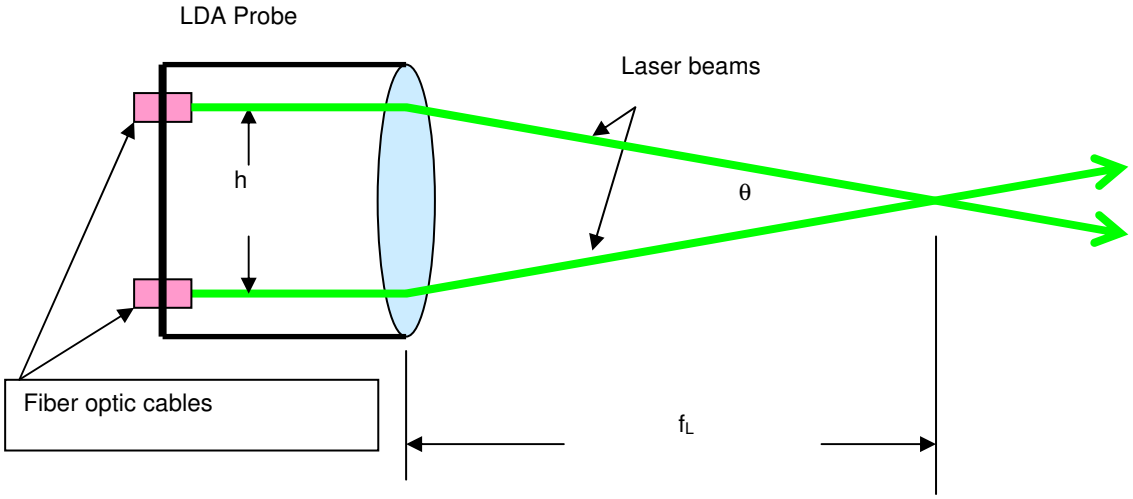

Figure 3 Laser Beams and Their Intersection Angle for 1D Component.

To resolve the sign of the velocity, a frequency offset generated by a Bragg cell is used to move the fringe

pattern through the sensing volume and across the scattering particle. As shown in Fig 3, fiber optic cables transmit laser light to the probe through a transmitter system. The transmitter system includes a color separator, beam splitter, and frequency shifter. The output ends of the optical cables are arranged at the fixed positions so the laser beams are parallel to the probe body.

The NIST LDA is a two velocity component system. The laser source is an Argon ion laser operated in multi-color mode. One velocity component uses green light (λ = 514.5 nm) and the second velocity component uses the blue light (λ = 488.0 nm). However, the green light component is used predominately, while the blue light component is used only occasionally for checking the system. Table 1 shows the nominal optical parameters of the LDA probe.

Table 1 Nominal Optical Parameters of the LDA Probe

Laser wavelength λ, nm	514.5
Laser beam separation *h*, mm	72.5
Focal length f_L, mm	1200
Beam intersection angle θ, deg.	3.46
Fringe spacing *d*, μm	8.52
Probe diameter d_m, mm	0.3
Probe length l_m, mm	9.9

In the context of airspeed measurement, the average frequency of the scattered light serves as the time scale. The droplet speed is determined by the LDA using the relation

$$V_{LDA} = d\ f_D \tag{3}$$

where f_D is the average Doppler frequency. NIST's LDA system uses a Dantec burst spectrum analyzer (BSA) to determine the Doppler frequency of the scattered light.

At NIST, the light scattering particles used for the airspeed measurements are water droplets injected from the fine air-water sprays located just upstream of the settling chamber of the wind tunnel, as shown in Figs. 1 and 2.

Spinning Disk Calibration of Laser Doppler Anemometer

In principle, the speed obtained from Eqn. (3) can be used as a primary standard for airspeed measurement if both the fringe spacing *d* (length scale) and the frequency f_D (time scale) are calibrated at specified uncertainty levels. The value of *d* can be accurately calculated from the laser wavelength λ and the beam angle θ if both θ and λ are calibrated. However, f_D, is determined by a BSA, which requires calibration to ensure the accuracy of the indicated Doppler frequency.

In this work, instead of measuring *d* and f_D separately, we calibrate the entire LDA system directly by comparing the speed indicated by the LDA to the known speed of a wire attached to a spinning disk unit [4], as shown in Figs. 4 and 5. Similar calibration techniques have been used by others. Dopheide, et al. [5] used the particles on the surface of a thick rotating glass wheel to generate the known tangential velocity. Kurihara, et al. [6] used a rotor with a single wire to simulate the trace particle. Park, et al. [7] used sand paper on a rotating disk to create a known velocity. At NIST, a 5 μm diameter wire is mounted on the rim of a disk of known diameter *D*. The disk and the light-scattering wire rotate at a measured rotation frequency f_{Disk}, thus enabling the calculation of the tangential speed of the wire from

$$V_{Disk} = f_{Disk}\ D/2 \tag{4}$$

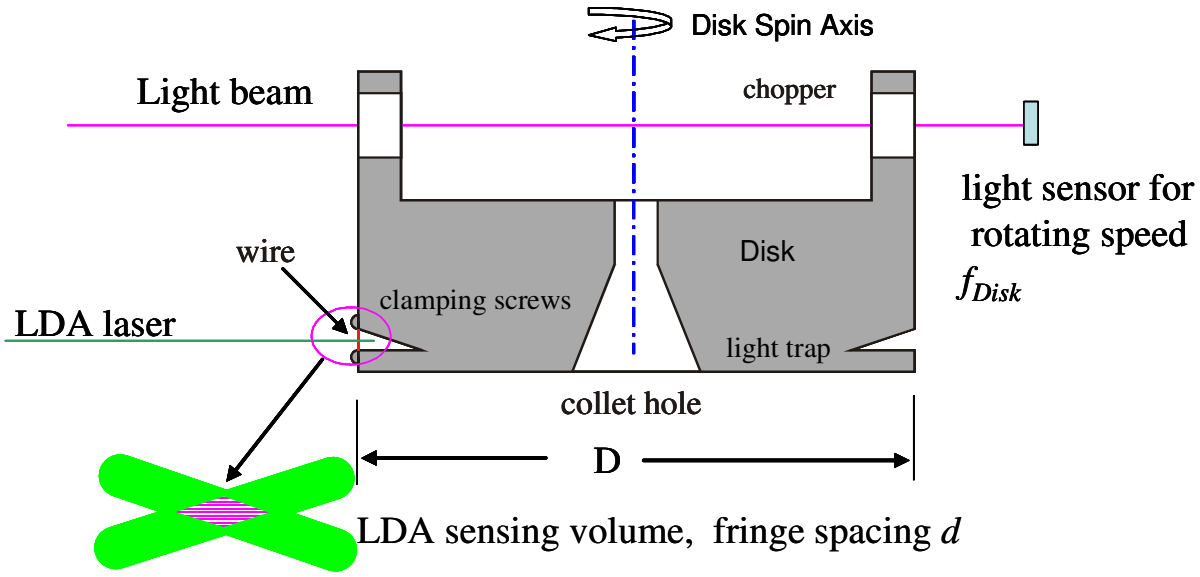

Figure 4 Schematic Diagram of the Spinning Disk for Calibrating the LDA.

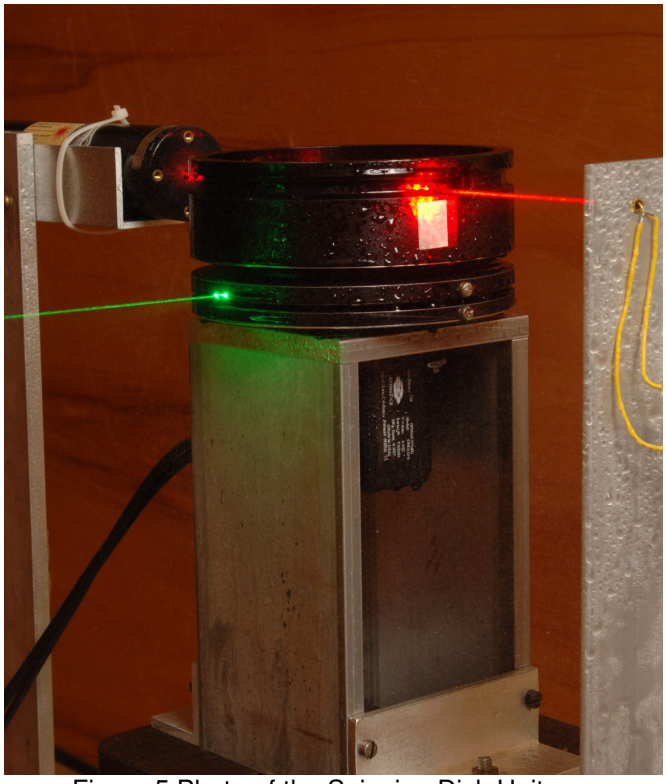

Figure 5 Photo of the Spinning Disk Unit.

The LDA is aligned so that the bisecting plane of the intersecting light beams is parallel to and passes through the axis of the disk and the wire passes through the intersection volume as the disk rotates. In this way, the LDA measures the known speed V_{Disk} produced by the spinning disk. The calibration factor, C_{LDA} is determined from the disk's speed and the speed indicated by the LDA using

$$C_{LDA} = \frac{V_{Disk}}{V_{LDA}} = \frac{D}{2}\,\frac{f_{Disk}}{f_D^C\; d} \tag{5}$$

where f_D^C is the frequency measured by the LDA system when it is scattering from the disk moving at the velocity V_{Disk}. The NIST standard speed thus becomes

$$V_{NIST} = C_{LDA}\; V_{LDA} = \frac{D}{2}\, f_{Disk}\, \frac{f_D}{f_D^C} \tag{6}$$

Thus, the NIST LDA airspeed system is traceable to the length (D) and time standards (f_{Disk}) used in the spinning disk calibration.

NIST LDA Airspeed Uncertainty Analysis

Below, we provide a detailed uncertainty analysis to show that the dominant uncertainties of the NIST air speed standard result from three items (1) uncertainty from the BSA, (2) fluctuations in the disk speed, and (3) misalignment of the intersecting laser beams. Items (1) and (2) are treated together. The third item is discussed separately. For completeness, the uncertainty analysis includes small terms that result from the frequency counter, the motor that turns the rotating disk, the thermal expansion of the rotating disk calibrator, the thermal expansion of the probe that supports the fiber-optic cables, misalignment of the LDA relative to the calibration velocity and misalignment of the LDA relative to the air flow when the LDA is used in the wind tunnel,

Here we follow the guidelines for evaluating and expressing uncertainty provided in NIST TN 1297 [8], the ISO Guide [9], and elsewhere [10]. According to [8], the sources of uncertainty used in assessing the combined standard uncertainty of the measurement process can be classified according to two types: *Type A* - those which are evaluated by statistical methods, and *Type B* - those which are evaluated by other means. Following this convention, each measured quantity has been classified accordingly as a u_A or u_B.

Referring to Eqn.(6), the airspeed uncertainty depends on the uncertainties of the variables of the diameter of the rotating cylinder D, the rotating frequency f_{Disk}, and the Doppler frequencies measured by the LDA system f_D^C and f_D. Although not shown in Eqn. (6) explicitly, many other variables could affect the uncertainties of the airspeed measurements. In addition, the result given in Eqn. (6) is based on the assumption of a perfect alignment. The misalignment of the LDA with disk will produced additional uncertainty.

Diameter of Rotating Disk, D

In the NIST facility, the light-scattering wire is a tungsten wire 5 μm in diameter. The wire is mounted by clamping screws to the curved surface of the short right circular cylinder shown in Figs. 4 and 5. The wire is parallel to the axis of the cylinder. The wire spans a groove machined into the cylinder, shaped to serve as a light trap to eliminate unwanted reflected laser light. A hole along the axis of the cylinder is shaped to receive a small collet to facilitate mounting the cylinder on the shaft of gear motors. Care was exercised in the machining process to assure that the collet hole and the curved surface of the cylinder are coaxial. The cylinder is mounted on the output shaft of a gear motor such that the cylinder rotates in a horizontal plane. The entire assembly is mounted on an *x-y* translation stage. The diameter of the cylinder was measured to be 136.522 mm with a standard uncertainty of 0.005 mm or 0.0037 % using a triple axis coordinate measuring machine. (See uncertainties in Table 2.) This will give 0.0037 % uncertainty in speed measurements.

Thermal Expansion of the Disk

The diameter of the disk *D* changes with the temperature. The temperature at which the diameter was measured might be different from the temperature where the diameter is used for LDA calibration. When the linear thermal expansion of the aluminum disk is assumed to be 2.3×10^{-5} /K, the change in *D* is 0.0126 mm or 0.0092 % for a 4 K difference in the temperature change. This contributes 0.0092 % uncertainty in speed.

Thermal Expansion of the Probe

As shown in Fig. 3, the separation of the laser beams *h* depends upon the dimensions of the LDA probe that supports two fiber optic cables. Although fringe spacing *d* is not explicitly shown in Eqn. (6), its uncertainty will affect the uncertainty of the burst frequency measurement. The dimension of the probe and the beam separation *h* and the fringe spacing *d* will change with the temperature. The housing of the probe is made from aluminum and the linear thermal expansion of the probe is assumed to be 2.3×10^{-5}/K. Referring to Eqns. (1) and (2), and the optical parameters of the probe given in Table 1, for a 4 K difference in temperature, the change in *h* is 0.0067 mm and in *d* is 0.00078 μm or 0.0092 %. Here, we have assumed that the temperature change does not affect the alignment of the two laser beams and that the beams are kept parallel to the probe body all the time. Since the uncertainty of *d* affects both the uncertainties of f_D^C and f_D, the total uncertainty on speed due to *d* is $\sqrt{2}$ x 0.0092 % = 0.013 %. Here the Type A variations of f_D^C and f_D are assumed to be independent.

Frequency Counter for the Rotating Disk

Calculation of the wire speed requires the measurement of the rotation frequency of the disk. This frequency is measured by counting the pulses produced by an optical signal modulated by the rotating disk. As shown in Fig. 4 or 5, the top surface of the disk was hollowed out so that the disk resembles a straight-sided bowl with a thick bottom. The side wall of the bowl has two holes, one centered on each end of a diameter through the axis. These holes serve as an optical chopper for a helium-neon laser, positioned so its light beam strikes a photo diode when the holes are aligned with the laser and the photo diode. This setup produces two pulses for each rotation. The output of the photo diode is counted with a frequency counter that determines the rotation rate of the disk. The frequency counter has a Type A uncertainty of 0.31 parts in 10^6 and a Type B uncertainty of 1.55 parts in 10^6. For a clock frequency of 1 MHz, this will give a Type A uncertainty of 3.2×10^{-5} % for a typical measurement time of 60 sec and Type B uncertainty of 0.0002 %.

Motor Speed Variation

An Animatics Smart Motor, Model SM2315D with Animatics power supply Model PS42V6AG-110 was used to drive the calibration disk. It provides stable rotation rates in very large rotating range and has an encoder with a resolution of 2,000 counts per revolution. The standard deviation of the disk rotation speed is found to be 0.038 % in the operation range.

Variation of Fringe Spacing with Position

When the Gaussian laser beam is focused by a lens, the minimum beam diameter (the waist) is found at the back focal plane of the lens only if a waist also exists at the front focal plane. Interference fringes are formed in the sensing volume where both laser beams intersect. Usually, the beam waists are not located exactly at this intersection; therefore, the sensing volume is enlarged and, as shown in Fig. 6, variably-spaced, curved, fringes result [2, 3]. The variable spacing leads to a significant error when the frequencies of the observed 'Doppler' signals are related to the speed of the scattering particles passing through the different parts of fringes.

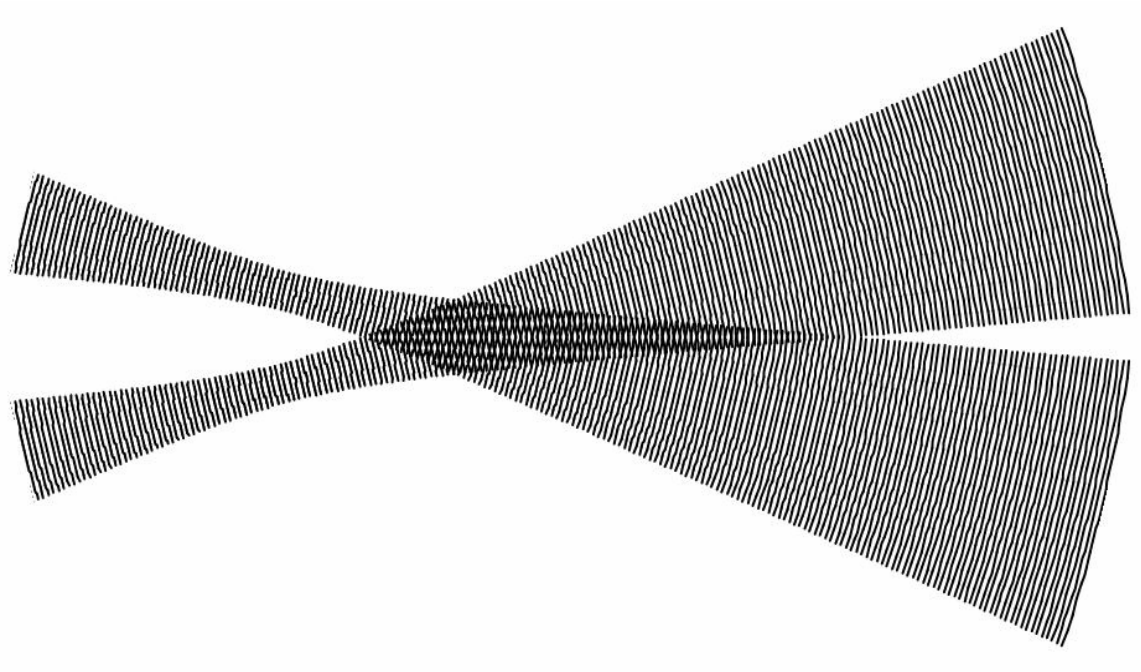

Figure 6 Fringe Spacing Variations in an Improperly Aligned System. Note the curved fringes in the sensing volume where the beams overlap.

When fringe spacing varies across the sensing volume, a constant wire speed will produce different LDA Doppler frequencies, depending upon the wire's location (See the value x_w in Fig. 9). Fig. 7 shows an example of the variation of the wire velocity indicated by the BSA as a function of the wire location. The indicated velocity is a linear function of the wire position within the sensing volume (-3 mm to +3 mm on Fig. 7) although the rotation speed was constant. Similarly, particles passing through different parts of the sensing volume will produce different speeds indicated by the LDA, even when their speeds are the same. In the NIST standard, the averaged speed indicated for all particles passing through the sensing volume is assumed to be the system speed for the LDA calibration. This assumption is reasonable because: (1) the variation of the speed ratio is linear, and (2) the particle concentration is uniform throughout the small sensing volume so the probability of the LDA signals produced by particles is symmetric about the center point.

To determine the mean value of the calibration, a least square error linear curve was obtained for each tested speed. The straight line shows the fitting of the data. From the fitted curve, both the mean value and the standard deviation of the LDA-disk calibration are obtained. The standard deviation obtained from the fitting will be discussed in the next section. The mean value is the speed calibration factor, C_{LDA} as described in Eqn. (5). The variation of the calibrated mean values are mainly due to the uncertainty of locating the wire position with respect to the probe volume. The standard deviation of this mean value is found to be 0.13%. This is classified as the uncertainty from the fringe space variation.

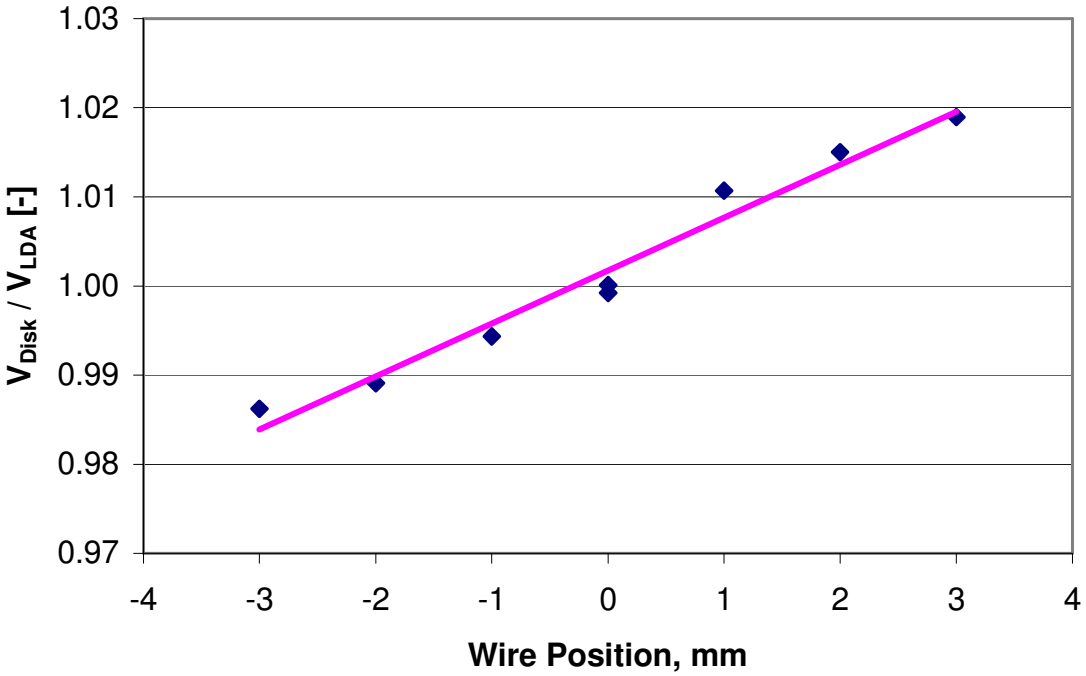

Figure 7 LDV Calibration Results vs Wire Position.

Burst Spectrum Analyzer, BSA

The frequency, f_D^C or f_D, is determined by a burst spectrum analyzer (BSA). The uncertainty of the BSA results from its internal clock (oscillator) and from the random and systematic uncertainties of the burst frequency calculated by the BSA. The sensitivity coefficients of f_D^C and f_D for airspeed are -1 and +1, respectively. Therefore, the systematic uncertainty of the BSA calculations will cancel out of the airspeed uncertainty while the random (Type A) uncertainty of the airspeed will be multiplied by the factor $\sqrt{2}$.

The clock used for the frequency or time scale has a Type A uncertainty of 0.5 parts in 10^6 and a Type B uncertainty of 2 parts in 10^6. For the nominal fringe space of 8.52 μm, the Type A and B uncertainties are 5×10^{-5} % and 0.0002 %, respectively. Thus the resulting uncertainty on speed due to the clock is $\sqrt{2}$ x 5×10^{-5} % $=7.1\times10^{-5}$ % for the Type A uncertainty and is zero for the Type B uncertainty due to cancellation.

The estimation of the other uncertainties for the BSA is more complicated. We have estimated these uncertainties from the uncertainty of the disk-LDA calibration. This uncertainty is identified by the standard deviation obtained from the curve fitting as discussed above and shown in Fig. 7. The uncertainty as a function of the calibrated speed is plotted in Fig. 8. Diamond symbols shown in Fig. 8 are the measured combined uncertainty of the disk-LDA calibration data. This uncertainty is mainly due to both the disk rotation speed and BSA uncertainties. Since the systematic uncertainty is cancelled out for the final speed measurement and is not the issue here, the data shown is only for the Type A uncertainty. These disk-LDA uncertainty data can be represented by two independent terms: a constant speed term and a constant ratio term. These two terms were found by fitting a curve to the data in Fig. 8 and the result of the fitting, $((0.13/V)^2 + (0.21)^2)^{1/2}$, in %, is shown as the solid curve. The constant speed term (the speed uncertainty for any speed) is 0.0013 m/s (corresponding to a 150 Hz on the BSA for an 8.52 μm fringe spacing) and the constant ratio term is 0.21 % of the speed. The constant speed term (0.0013 m/s) results from the resolution of the BSA while the constant ratio term results from the combined effect of the motor speed variation and the noise of the BSA.

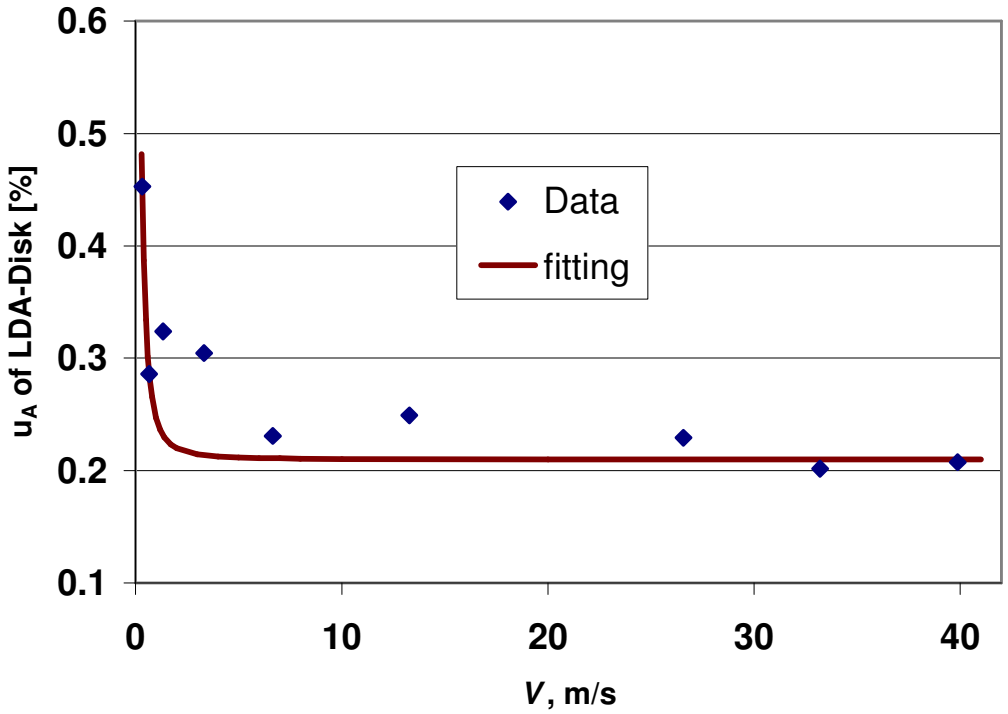

Figure 8 Type A Uncertainty of LDA-Disk Calibration. The fitting is $((0.13 / V)^2 + (0.21)^2)^{1/2}$ in %.

The BSA uncertainty can be estimated by subtracting the motor speed uncertainty of 0.038 %, found above, from the combined uncertainty (accounting for the RSS relationship). Here we have assumed that the motor speed uncertainty is independent of the BSA uncertainty. The resulting BSA uncertainty for the constant percentage term is thus 0.207 % (= $(0.21^2 - 0.038^2)^{1/2}$ %). It is the uncertainty of the conversion factor of the BSA.

The Type A uncertainty of the BSA affects both f_D^C and f_D independently and thus the resulting speed uncertainty is $\sqrt{2}$ x 0.0013 m/s = 0.0018 m/s for the constant speed term and $\sqrt{2}$ x 0.207 % = 0.29 % for the constant percentage term.

Angle Misalignment for LDA-Disk Calibration

As noted above, the result given in Eqn. (6) is based on the assumption of a perfect alignment. The misalignment of the LDA and disk will produce additional uncertainty. The rotating disk is mounted on the output shaft of a gear motor such that the disk rotates with a vertical spin axis. The entire assembly is mounted on an *x-y* translation stage. The alignment of LDA probe with the direction of the wire velocity is another parameter to be examined. As noted above, the LDA must be aligned so that the plane bisecting the intersection angle is parallel to and passes through the axis of the cylinder. Fig. 9 shows the local coordinates for the disk and the laser beams intersection during the LDA-Disk calibration. The laser beams define an *x-y* plane and *z* is normal to the *x-y* plane. The center of the sensing volume is chosen to be the coordinate origin, (0,0,0). The light scattering wire is located at x_W, oriented in the *z* direction and moves in the *y* direction when the disk is rotating. ***n*** is a unit vector normal to the bisecting plane (*x-z* plane). The fringes are parallel to the bisecting plane. ϕ is the angle between the wire velocity V_{DISK} and the unit vector, ***n***. *C* is the axis of the rotating disk.

To align the LDA with the disk, an acrylic rod is mounted vertically in the hole on top of the collet of the disk. The LDA is aligned with the axis by *x-y* translations of the cylinder assembly so that the intersection volume is centered on the axis of the acrylic rod (*C* in Fig. 9). A 1 mm diameter hole was drilled along the axis of the rod. When a laser beam intersects the axis, the hole scatters light making the laser visible. The *x-y* translation stage supporting the rotating disk is adjusted to maximize the scattered light. Then, the translation stage supporting the fiber optic probe is backed away from the disk a distance equal to the radius of the cylinder and the probe is lowered so that the wire passes through the sensing volume. To ensure the bisecting plane of the laser beams passes through the disk's axis when the traversing system is moved, the bisector of the laser beams (the optical probe) must be correctly aligned with the translation stage. Final adjustment is done by turning the lead screw of the translation stage slowly while watching the input to the signal processor on an oscilloscope.

When the LDA system is misaligned with respect to the calibration system by the angle ϕ, the observed speed is $V_{Disk}\cos(\phi)$. The misalignment angle ϕ can be decomposed into two orthogonal angles, ϕ_x and ϕ_z. The misalignment angles ϕ_x and ϕ_z are estimated to be less than 0.5 deg. Thus, each angle contributes a speed uncertainty of 0.004 %.

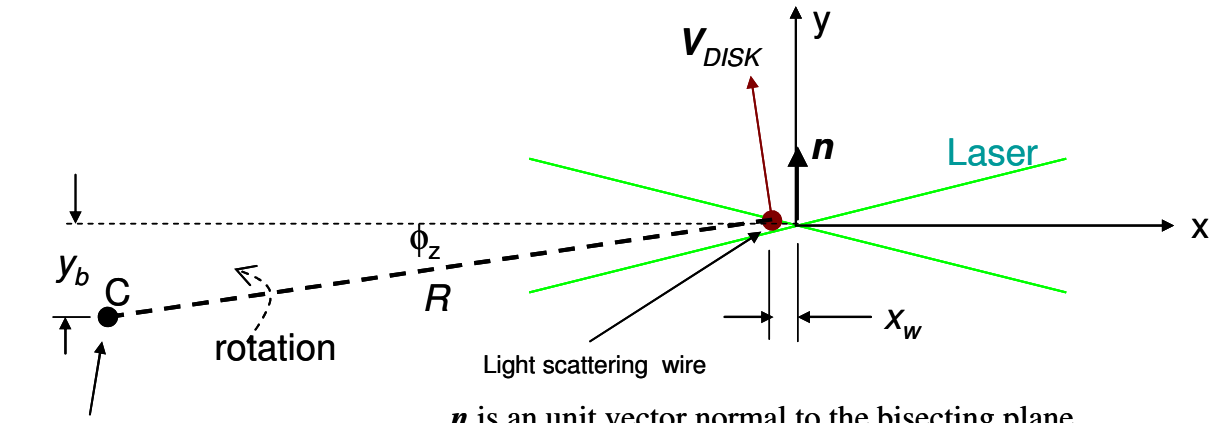

Figure 9 Local Coordinates for the Spinning Disk and the Laser Beam Intersection.

Misalignment in LDA with Wind Tunnel Installation

The sources of the uncertainties discussed above are only for the LDA airspeed standards system. However, additional uncertainties must be added if the LDA probe is not aligned with respect to the airspeed direction in the test section of the wind tunnel or if the device under test is misaligned. Ideally, the unit vector of the bisecting plane should be in the direction of the airspeed (*y)*. That is, the laser bisecting plane should be in vertical direction (*z*) and parallel to the *x* direction (horizontal and normal to *y*). α_x and α_z denote the angles of misalignment rotated around the *x* and *z* axes, respectively. The airspeed uncertainty due to the cosine effect varies with 1-cos(α_x) and 1-cos(α_z). The uncertainties of these misaligned angles are estimated to be 1 deg. and thus a speed uncertainty of 0.015 % for both α_x and α_z.

Summary of the NIST Airspeed Standards Uncertainty

Table 2 lists the sources and values of the uncertainties and the effect of the source uncertainties on the uncertainty of the NIST airspeed standards. As shown in Table 2, the major uncertainty of the airspeed standards is due to the BSA uncertainty and the variation of fringe spacing.

The airspeed uncertainty is classified into two types: a constant speed term and a constant percentage term as shown in Table 2. The uncertainty for each group is then combined and given in Table 3.

Based on the data in Table 3, the results for the total combined standard uncertainty for the NIST airspeed, in m/s can be given as

$$u_c(V_{NIST}) = \sqrt{(0.0029 V_{LDA})^2 + (0.0013 V_{LDA})^2 + (0.0018)^2} \quad (7)$$

where V_{LDA} is in m/s. The approximate confidence level of the result given above is 68 %. Following the guidelines of [8], the expanded uncertainty with a coverage factor k is given as

$$U(V_{NIST}) = k\sqrt{(0.0032\, V_{LDA})^2 + (0.0018)^2} \quad (8)$$

When a coverage factor of $k = 2$ is used to convert the combined standard uncertainty to an expanded uncertainty, with an approximate 95 % level of confidence, the expanded uncertainty, in m/s, becomes:

$$U(V_{NIST}) = \sqrt{(0.0064\, V_{LDA})^2 + (0.0036)^2} \quad (9)$$

Table 2 Summary of Sources and NIST Airspeed Uncertainties.

Variable Sources	Sources			Speed Uncertainty	
	Mean	u_A	u_B	u_A %	u_B %
Diameter of rotating disk, D [mm]	136.5	0	0.005	0	0.0037
Thermal expansion of D, [mm]	136.5	0.0126	0	0.0092	0
Fringe spacing expansion, d [μm]	8.52	0.0008	0	0.013	0
Timer for rotating disk [parts in 10^6]	~	0.31	1.55	3.2×10^{-5}	0.0002
Rotation speed, [%]	~	0.038	0	0.038	0
Fringe spacing with position, [%]	~	0	0.13	0	0.13
Clock for BSA [parts in 10^6]	~	0.5	2.0	7.1×10^{-5}	0
BSA constant speed term [m/s]	~	0.0013	0	$0.18/V_{LDA}$	0
BSA constant ratio term [%]	~	0.207	0	0.29	0
LDA-disk, ϕ_x , [deg]	0	0	0.5	0	0.004
LDA-disk, ϕ_z , [deg]	0	0	0.5	0	0.004
LDA-wind tunnel, α_x, [deg]	0	0	1.0	0	0.015
LDA-wind tunnel, α_y , [deg]	0	0	1.0	0	0.015

Table 3 Combined Airspeed Uncertainty

	u_A %	u_B %
Constant ratio term	0.29	0.13
Constant speed term	$0.18/V_{LDA}$	0

Based on Eqn. (9), the NIST airspeed expanded uncertainty is plotted in Fig. 10 in the unit of m/s for the coveraged airspeed range of 0.15 m/s to 40 m/s. This gives a minimum uncertainty of 0.0038 m/s at the lowest airspeed of 0.15 m/s and a maximum uncertainty of 0.26 m/s at the highest speed of 40 m/s. The same uncertainty data are plotted in Fig. 11 in the unit of %. This gives a maximum uncertainty of 2.5 % at the lowest airspeed of 0.15 m/s and a minimum uncertainty of 0.65 % at the highest speed of 40 m/s.

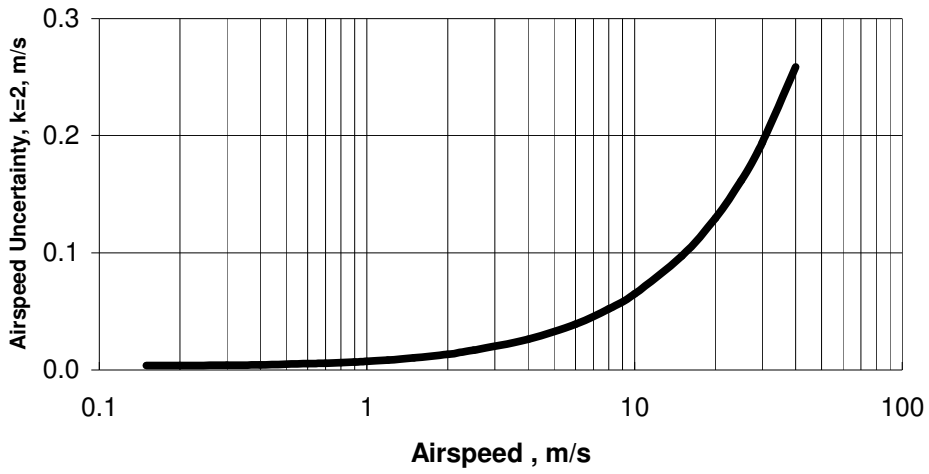

Figure 10 NIST Airspeed Uncertainty in m/s versus Airspeed

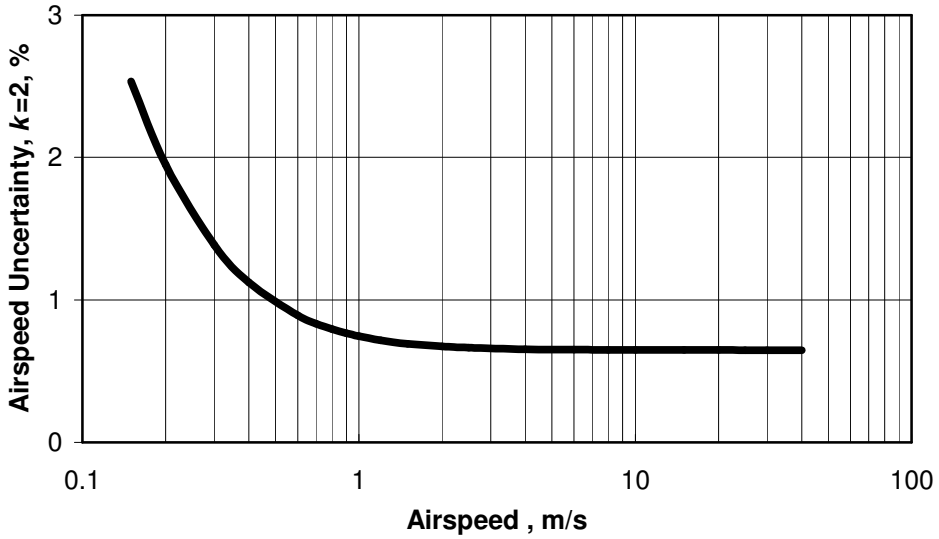

Figure 11 NIST Airspeed Uncertainty in % versus Airspeed

Acknowledgments

The authors gratefully acknowledge the technical assistance of Drs. J.D. Wright and M.R. Moldover.

References

[1] Mease, N.E., Cleveland, W.G., Mattingly, G.E. and Hall, J.M., "Airspeed Calibrations at the National Institute of Standards and Technology", Proceedings of the Measurement Science Conference, Anaheim, CA 1992.

[2] Durst, F., Melling, A. and Whitelaw, J.H. "Principles and Practice of Laser-Doppler Anemometry", Academic Press, NY, 1976

[3] Thompson, H. and Stevenson, W.H. "Laser Velocimetry and Particle Sizing", Hemisphere Publishing Corporation, NY, 1979

[4] Bean, V.E. and Hall, J.M., "New Primary Standards for Air Speed Measurement at NIST", Proceeding of the 1999 NCSL Workshop and Symposium, Charlottle, NC.
[5] Dopheide, D., Taux, G. and Narjes, L. "Accurate Flow Rate Measurements by Means of Laser Doppler Anemometry", 3rd Conference of the IMEKO Technical Committee on Flow Measurements TC9, FLOMEKO '83, September 20 - 22, 1983, pp. 51-59
[6] Kurihara, N., Terao, Y. and Takamoto, M. "LDV Calibrator for the Air Speed Standard between 1.3 to 40 m/s", 5th International Symposium on Fluid Flow Measurement, Arlington, Virginia April 2002
[7] Park, J.T., Cutbirth, J.M. and Brewer, W.H. "Hydrodynamic Performance of the Large Cavitation Channel", 4th ASME_JSME Joint Fluids Engineering Conference, Honolulu, Hawaii, July 2003
[8] Taylor, B. N., and Kuyatt, C. E., Guidelines for Evaluating and Expressing the Uncertainty of NIST Measurement Results, NIST Technical Note 1297, 1994 Edition, National Institute of Standards and Technology, Gaithersburg, Maryland.
[9] International Organization for Standardization (ISO), “Guide to Expression of Uncertainty in Measurement, Geneva, Switz., 1993 edition.
[10] Coleman, H. W. and Steele, W. G., “Experimentation and Uncertainty Analysis for Engineers,” 2nd ed., John Wiley and Sons, NY, 1999.